

Pinco: Position-induced Consistent Adapter for Diffusion Transformer in Foreground-conditioned Inpainting

Guangben Lu^{1,2,*} Yuzhen Du^{1,*} Zhimin Sun¹ Ran Yi^{1,✉} Yifan Qi²
 Yizhe Tang¹ Tianyi Wang² Lizhuang Ma¹ Fangyuan Zou²

¹Shanghai Jiao Tong University ²Tencent

{Haaaaaaaaa, zhimin.sun, ranyi[✉], tangyizhe}@sjtu.edu.cn ma-lz@cs.sjtu.edu.cn

{lucasgblu, ivanqi, joshtywang, ericfyzou}@tencent.com

* Equal contribution ✉ Corresponding author

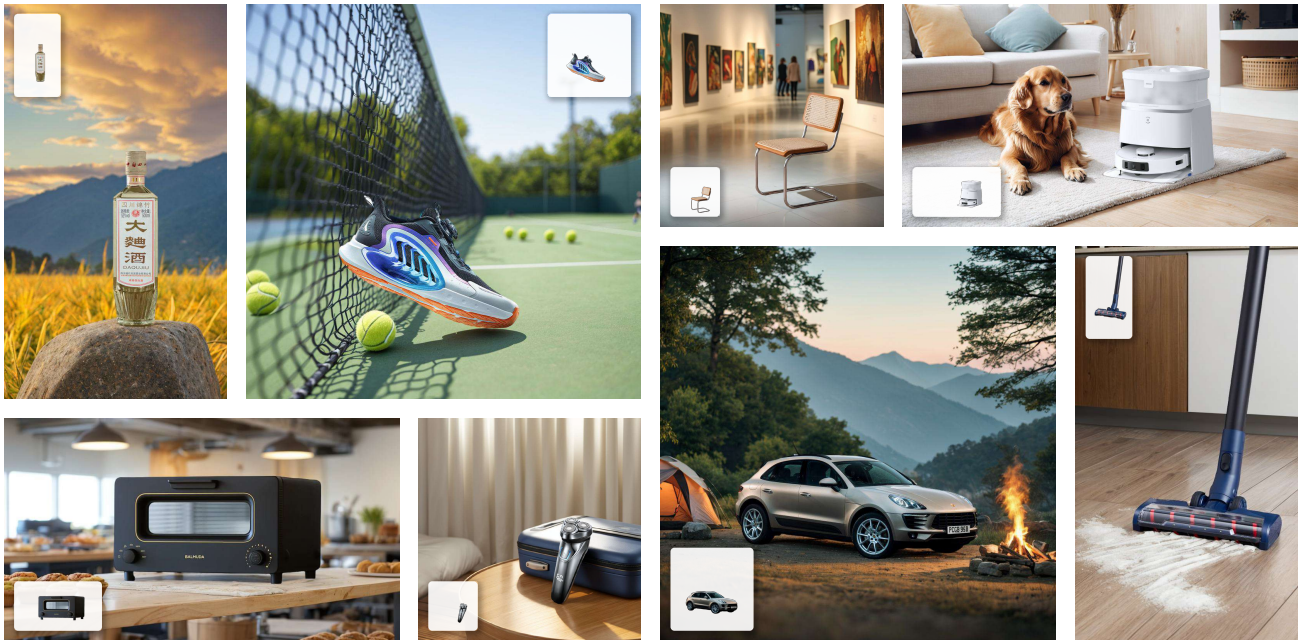


Figure 1. Photorealistic samples generated by Pinco, exhibiting its outstanding capabilities in foreground consistency preservation, rational spatial arrangements, and diverse background generation.

Abstract

Foreground-conditioned inpainting aims to seamlessly fill the background region of an image by utilizing the provided foreground subject and a text description. While existing T2I-based image inpainting methods can be applied to this task, they suffer from issues of subject shape expansion, distortion, or impaired ability to align with the text description, resulting in inconsistencies between the visual elements and the text description. To address these challenges, we propose Pinco, a plug-and-play foreground-

conditioned inpainting adapter that generates high-quality backgrounds with good text alignment while effectively preserving the shape of the foreground subject. Firstly, we design a Self-Consistent Adapter that integrates the foreground subject features into the layout-related self-attention layer, which helps to alleviate conflicts between the text and subject features by ensuring that the model can effectively consider the foreground subject’s characteristics while processing the overall image layout. Secondly, we design a Decoupled Image Feature Extraction method that employs distinct architectures to extract semantic and shape features

separately, significantly improving subject feature extraction and ensuring high-quality preservation of the subject’s shape. Thirdly, to ensure precise utilization of the extracted features and to focus attention on the subject region, we introduce a Shared Positional Embedding Anchor, greatly improving the model’s understanding of subject features and boosting training efficiency. Extensive experiments demonstrate that our method achieves superior performance and efficiency in foreground-conditioned inpainting.

1. Introduction

Visual generative models [10, 39] have made significant progress recently and have demonstrated exceptional potential in various applications, including image editing [20, 24], image restoration [23, 30], and virtual reality. Among these applications, a notably promising yet challenging task is foreground-conditioned inpainting. This task focuses on generating high-quality backgrounds based on a provided text description while maintaining the integrity of the given foreground subject. It is closely related to the conventional text-guided image inpainting task [10, 21, 39, 53], which involves inpainting content within a small region based on a brief text description. However, the foreground-conditioned inpainting task presents greater challenges due to the following reasons: 1) It requires inpainting a larger area (the background region) with a more complex text description, and 2) It is crucial to preserve the integrity of the foreground subject’s shape while ensuring harmonious coordination between the foreground subject and the background. To address these challenges, we propose Pinco, an innovative solution that effectively improves the performance of foreground-conditioned inpainting.

Conventional text-guided image inpainting methods based on T2I diffusion models can be classified into three categories: 1) Sampling modification methods [2, 3, 10, 12, 31, 50], which adjust the diffusion sampling strategy to achieve inpainting, such as through latent space replacement. While these methods can be seamlessly adapted to various diffusion backbones, they may disrupt the original latent distribution, leading to irrational layout compositions or unreasonable object placements (Fig. 2). 2) Model fine-tuning methods [36, 47, 53], which typically involve modifying the network structure of pre-trained T2I models and utilizing relatively small-scale datasets. These methods can cause the model to forget pre-trained knowledge and make it prone to fitting the distribution of the fine-tuned training dataset, ultimately affecting the quality and diversity of the generated images. 3) Conditional injection methods [1, 13, 18, 21, 49], which incorporate information from the preserved region into the frozen T2I model via a side-branch mechanism. Most of these methods [1, 18, 21] employ the ControlNet [49] structure, replicating half or the

entire T2I model for inpainting injection. However, as the scale of the T2I model increases, these side-branch models become increasingly cumbersome and impractical to implement. Additionally, adding extra control information after the completion of text cross-attention may result in a decline in text-image consistency.

To address these issues, we propose **Pinco**, a powerful yet efficient plug-and-play adapter that empowers DiT-based models for consistent foreground-conditioned inpainting. We design three innovative modules: 1) **Self-Consistent Adapter**. To effectively inject the subject features into the base model, we build our injection method based on the concept of image prompt adapter [48], which conventionally injects the subject feature through cross-attention layer and integrates it with the text cross-attention in the base model. However, such integration by directly adding outputs of subject cross-attention and text cross-attention can easily cause conflicts between text and the injected subject information, resulting in a mismatch between the text and generated background. Therefore, we propose a Self-Consistent Adapter, which makes an innovative shift by integrating subject cross-attention into the self-attention layer, effectively alleviating the conflicts between text and subject features. 2) **Decoupled Image Feature Extraction**. The conventional feature extractors, CLIP and VAE Encoder, used in controllable T2I models are both suboptimal for our subject feature extraction: the CLIP encoder only captures abstract global semantic information, while the VAE encoder provides a limited amount of shape features, which is insufficient to meet the requirements of strict contour preservation in our task. To address these issues, we propose a novel semantic-shape decoupled extractor, using different architectures for semantic and shape features extraction from different sources, ensuring effective extraction of subject features with fine details of subject shape, achieving high-quality preservation of the subject outline and effectively avoiding expansion. 3) **Shared Positional Embedding Anchor**. To ensure the precise utilization of subject features, attention in subject cross-attention should be concentrated in the subject region. In light of this, we propose a Shared Positional Embedding Anchor that combines positional embeddings with subject features prior to the calculation of subject cross-attention. This approach achieves a decay in attention weights as the distance from the subject region increases, thereby concentrating attention inside the subject region. This operation greatly enhances the model’s understanding of subject features and improves training efficiency. Extensive experiments demonstrate that our method achieves superior foreground-conditioned inpainting performance and efficiency.

We summarize our contributions in four-fold:

1. We propose Pinco, a powerful yet efficient plug-and-play adapter that can be seamlessly integrated with DiT-based

models to achieve high-quality foreground-conditioned inpainting. With a small number of training parameters, it only increases negligible inference latency compared to the base model, while ensuring the high-quality generation of rich and diverse backgrounds.

2. We propose Self-Consistent Adapter, a mechanism that injects subject feature through cross-attention, and innovatively integrates this subject cross-attention into the self-attention layer of the base model, effectively alleviating the conflicts between text and subject features.
3. We propose a Decoupled Image Feature Extraction strategy, which decouples the extraction of the semantic and shape features of the subject, ensuring effective extraction of subject features with fine details of subject shape, and enhancing the preservation of the subject shape.
4. We propose a Shared Positional Embedding Anchor, which combines positional embedding with subject features before attention calculation to constrain the activated region in the subject cross-attention, ensuring precise utilization of subject features.

2. Related Work

2.1. Controllable Image Generation

There are various approaches to control generative diffusion models, some of which may represent promising directions for subject-driven, prompt-guided image synthesis. Certain methods [9, 17, 32, 40] achieve personalization by individually fine-tuning for each given subject. Despite their success, these methods require re-tuning to each new concept and fail to maintain the exact details of the subject. To address these challenges, some methods [11, 15, 33, 48, 49] reuse certain modules of the base model to achieve general feature extraction from reference images, and inject these extracted features into the frozen base model without subject-specific tuning. However, as the scale of the T2I models increases, these methods become increasingly impractical. In contrast, IP-Adapter [48] utilizes a lightweight decoupled attention mechanism to incorporate semantic features of the reference subject into the model. Another methods [7, 19, 28, 29] directly alter the attention map during sampling to facilitate subject generation, which carries the risk of compromising the inherent textual coherence.

2.2. Image Inpainting for Foreground Condition

With the impressive performance of T2I diffusion models [16, 34, 36, 39] in image generation, a variety of diffusion-based inpainting methods [10, 21, 39, 53] have been proposed. 1) some methods [2, 3, 10, 12, 50] utilizes a classic unmask region copying strategy, replacing known areas with the original image during the diffusion model’s inference. However, this approach is rigid and of-



Figure 2. Foreground-conditioned inpainting results of three existing T2I Inpainting methods, Pixart- α (sampling strategy modification), SDXL-Inpainting (Model fine-tuning), BrushNet (Conditional injection), and ours. Existing methods suffer from issues such as shape expansion and unreasonable spatial relationships between the foreground subject and background.

ten overlooks the semantic information of the foreground subject, causing shape expansion problems. 2) To avoid this problem, some methods [31, 47, 53] ensure the preservation of the subject by modifying and fine-tuning the model. PowerPaint [53] fine-tunes a text-to-image model with two learnable task prompts to achieve the subject semantic understanding. However, this approach can be challenging to train and may compromise the model’s inherent text-to-image capabilities, leading to unalignment between the generated background and the input text. 3) Other methods [13, 18, 21, 49] inject the information of known area by side-branch injection. BrushNet [21] adopts a hierarchical approach by gradually incorporating the full UNet feature layer-by-layer into the pre-trained UNet. These ControlNet-style methods have extensive training parameters, and the pattern of injecting features after text cross-attention can lead to a deterioration of text alignment, as the visual features may dominate the generation. To address these challenges, we propose Pinco, a plug-and-play and lightweight adapter method, which requires very few parameters while efficiently injecting the characteristics of the subject.

3. Preliminaries

3.1. Diffusion Models

The diffusion models [38] encompass forward and reverse processes. In the forward diffusion process, a noise is added to a clean image x_0 in a closed form. In the reverse process, given input noise x_T sampled from a random Gaussian distribution, a trainable network ϵ_θ estimates the noise at each step t conditioned on c . The diffusion model training process aims to optimize the denoising network ϵ_θ so that it can accurately predict the noise given the condition c :

$$\mathcal{L} = \mathbb{E}_{x_0, c, \epsilon \sim \mathcal{N}(0,1), t} [\|\epsilon - \epsilon_\theta(x_t, t, c)\|_2^2]. \quad (1)$$

In foreground-conditioned inpainting scenario, the condition c includes detailed text descriptions as well as independent foreground regions.

3.2. Diffusion Transformer (DiT)

Our Pinco is built upon the open-source Hunyuan-DiT [25], which is an enhanced version of the DiT model [35]. The

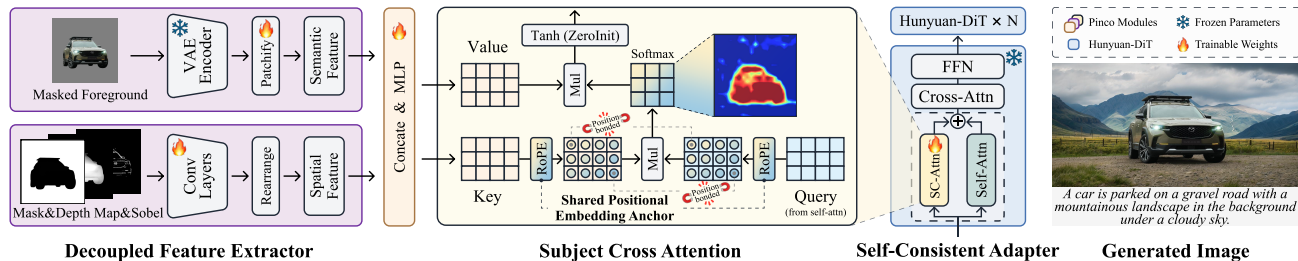


Figure 3. The framework of our **Pinco**, a plug-and-play inpainting adapter that can be seamlessly integrated with a text-to-image DiT model for consistent foreground-conditioned inpainting. Pinco consists of three modules: A **Decoupled Feature Extractor** used to extract subject feature, a **Shared Positional Embedding Anchor** used to ensure foreground attention, and a **Self-Consistent Adapter** injecting subject feature on the self-attention layer.

DiT model is a transformer-based diffusion method that operates on latent patches with a series of transformer blocks (DiT Blocks). Notably, the DiT Block enhances standard normalization layers with adaptive layer normalization (AdaLN). Hunyuan-DiT further utilizes cross-attention mechanism for fine-grained text understanding similar to Stable Diffusion [39]. Additionally, Hunyuan-DiT incorporates Rotary Positional Embedding (RoPE) [41], which captures both absolute and relative positional dependencies and introduces a two-dimensional RoPE to extend its functionality to the image domain

4. Method

Overview. Pinco is a plug-and-play inpainting adapter that can be seamlessly integrated with a text-to-image DiT model to enable consistent foreground-conditioned inpainting. The inputs to our inpainting system consist of a subject image, a mask image, and a text prompt (describing the desired background), with the subject depth image and Sobel image as conditioning signals. Pinco aims to inpaint the background region so that the generated background is consistent with the text description and natural, while the foreground subject remains unchanged.

Fig. 3 shows the framework of our Pinco and the base DiT model. Pinco first extracts the semantic and shape features of the subject image through a **Decoupled Image Feature Extractor** (Sec. 4.2). Then Pinco injects the extracted subject feature into the base model through a novel **Self-Consistent Adapter** (Sec. 4.1), which designs a subject cross-attention to inject subject features, and innovatively integrates it into the self-attention layer of the base model. Before the subject cross-attention calculation, Pinco uses a novel **Shared Positional Embedding Anchor** (Sec. 4.3), that combines positional embedding with subject feature to constrain the activated area in the subject cross-attention to the subject region. After the subject information is effectively injected and utilized, we employ the diffusion denoising of the base model to generate high-quality backgrounds.

4.1. Self-Consistent Adapter

In foreground-conditioned inpainting, the features of the foreground subject need to be injected into the base T2I diffusion model. Classical methods for adding image conditions in T2I models can be categorized into three main approaches: 1) Concatenating all images and expanding the model’s input channels, which requires significant training overhead for fine-tuning. 2) Creating a side branch injection by copying part of the base model (*e.g.*, ControlNet [49]), which adds many parameters and can slow down inference. 3) Training a lightweight and effective image prompt adapter [27, 43]. We build our subject feature injection method on the concept of the image prompt adapter.

Previous image prompt adapters [44, 48] typically integrate image features with the text cross-attention layer. A naïve way is to adapt the decoupled cross-attention mechanism in these works to our task, designing a **subject cross-attention** (cross-attention between the latent and subject features) for injecting subject image features, along with a text cross-attention, and integrating these two cross-attention layers by adding their outputs. However, using this approach can lead to a disharmonious result. Since the text is often complex and primarily about the background, such integration can cause conflicts between text features and subject features, resulting in: 1) subject outward expansion or distortion in the generated image; and 2) a mismatch between the text and the generated background.

To tackle these challenges, we draw inspiration from the analyses of cross-attention and self-attention presented in previous works [27, 43], which show that the self-attention map can be effectively leveraged to preserve the spatial structural characteristics of the original image. This observation indicates that self-attention is more closely aligned with the layout of the final output, thereby presenting a promising pathway for enhancing the results of foreground-conditioned inpainting. Building on this understanding, we propose **Self-Consistent Adapter**, making an innovative shift by *integrating subject cross-attention directly into the self-attention layer*. This approach avoids the conflict be-

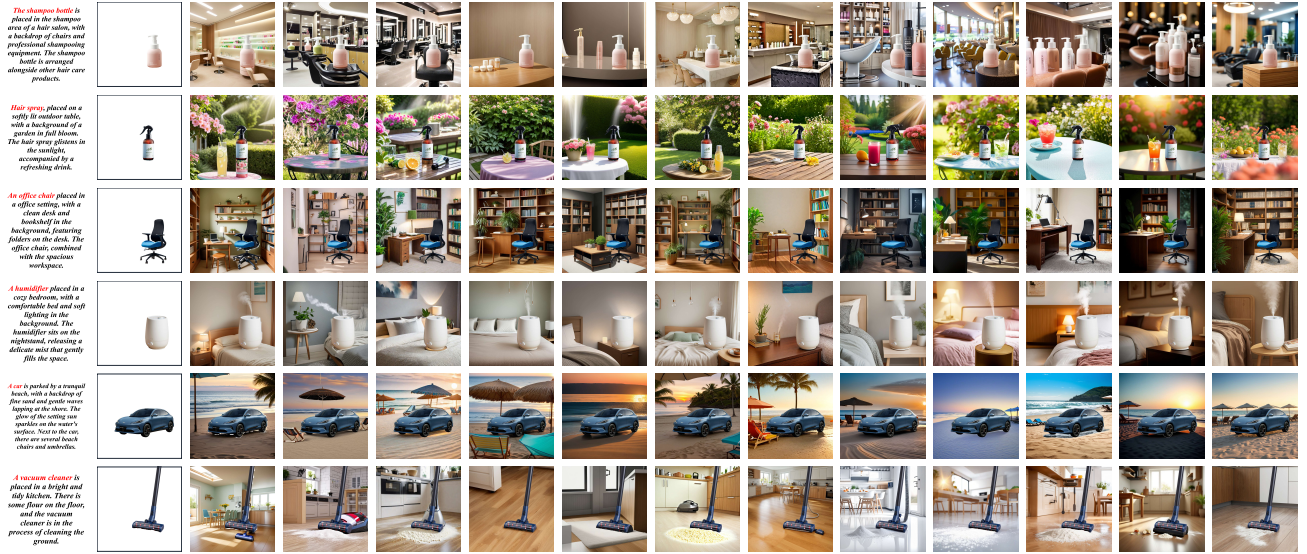


Figure 4. Quantitative Comparison of previous inpainting methods and our *Pinco*. Our method is capable of generating coherent, detailed and rational backgrounds following the provided text, while effectively mitigating the problem of subject expansion

tween subject features and text, allowing for better preservation of the subject shape in the generated image, and maintaining the alignment between the background and text. The modified attention mechanism can be expressed mathematically as follows:

$$Z = \alpha \text{Softmax}\left(\frac{QK^T}{\sqrt{d}}\right)V + \beta \text{Softmax}\left(\frac{Q(K_{sub})^T}{\sqrt{d}}\right)V_{sub}, \quad (2)$$

where α and β are parameters used to tune the injection strength, Q is the query, K, K_{sub}, V and V_{sub} are the key and value calculated from latents and subject feature. We also use Zero-init Tanh Gating [51] to progressively control the strength of injecting features into the base model.

4.2. Decoupled Image Feature Extractor

For T2I-model-based foreground-conditioned inpainting, the features of the foreground subject need to be extracted and injected into the base model, where the subject feature is commonly extracted from the concatenation of the subject image, the mask image and other images related to the subject (e.g., depth map and Sobel image). The image feature extraction of controllable T2I models primarily relies on CLIP or VAE encoder. Due to the inherent network structure and training strategy, the CLIP image encoder primarily captures high-level global semantic information of the overall image. Compared to CLIP, the VAE encoder is capable of extracting more shape information. However, it is still challenging for VAE, commonly used in many inpainting methods [21, 36, 53], to meet the requirements of strict contour preservation in our task. Therefore, we propose a Semantic-Shape Decoupled Image Feature Extrac-

tor to ensure the sufficient extraction of both semantic and shape information of the given subject.

Our Semantic-Shape Decoupled feature extractor consists of three parts: semantic feature extraction, shape feature extraction, and feature fusion. **1) Semantic Feature Extraction.** The semantic and textural features of the subject are mainly extracted from the 3-channel (RGB) subject image (with background removed). To align the extracted feature with the data distribution of the pre-trained diffusion model, we reuse the original VAE encoder as the semantic feature extractor, which reduces the overhead of additional training. **2) Shape Feature Extraction.** It is crucial to maintain the details of the subject’s shape in foreground-conditioned inpainting. Inaccurate shape feature extraction can lead to the expanding of the subject shape in the output image. Therefore, to accurately extract subject shape features, we leverage the subject’s mask, depth map, and Sobel images to supplement the shape details of the subject. To ensure effective extraction of the local shape details, we construct a convolutional feature extractor to extract shape features. **3) Feature Fusion.** After extracting semantic and shape features, both features are channel-wise concatenated together, and an MLP module is used to fuse these two features afterwards.

Through this decoupled feature extraction method, we can not only fully utilize the information contained in the provided condition images, but also extract fine details of the subject shape, thereby significantly reducing the outward expansion of the subject shape in the output image.

4.3. Shared Positional Embedding Anchor

Table 1. Quantitative comparison between Pinco and previous methods. Pinco demonstrates the best subject shape preservation and text alignment effects, while also having very few training parameters.

Architecture	Metrics	Model Characters	Image Quality	Foreground Consistency			Text Alignment		Rationality
	Methods			TPR	FID ↓	OER(SAM2.1) ↓	OER(BiRefNet) ↓	LPIPS ↓	
UNet	SD1.5 + ControlNet Inpainting	29.59%	84.28	22.00%	52.28%	0.008555	0.849	22.83%	4.012
	HD-Painter	0.00%	88.75	22.04%	37.56%	0.007171	0.813	13.26%	4.624
	LayerDiffusion	24.67%	107.98	20.31%	27.81%	0.007996	0.864	17.34%	4.358
	BrushNet-SD1.5	41.86%	84.16	19.60%	36.19%	0.005779	0.868	19.67%	4.335
	BrushNet-SDXL	12.69%	87.00	28.25%	18.91%	0.005776	0.870	9.83%	4.621
	PowerPaint V2	0.06%	88.52	33.80%	44.89%	0.010514	0.801	22.74%	4.669
	SDXL inpainting	100.00%	83.60	25.24%	30.77%	0.007946	0.847	13.96%	4.536
	Kolors inpainting	100.00%	85.59	21.47%	14.40%	0.004223	0.891	5.27%	4.418
DiT	SD3-medium Controlnet Inpainting	49.94%	98.91	28.98%	31.11%	0.004553	0.912	12.55%	4.592
	Flux-dev Controlnet Inpainting Beta	15.25%	111.91	28.11%	22.30%	0.004502	0.916	13.17%	4.629
	Pinco-Self	11.37%	84.25	11.51%	10.00%	0.004441	0.901	3.16%	4.790

After obtaining a high-quality subject feature from the decoupled image feature extractor (Sec. 4.2), we use a subject cross-attention layer to fuse the subject feature with the latent feature, which is then integrated with self-attention layer by Self-Consistent Adapter (Sec. 4.1). However, we observe that when the subject feature is directly fed into the subject cross-attention without incorporating positional embeddings, the attention tends to disperse into regions that resemble the texture and content of the subject (Fig. 7). This leads to a situation in the generated images where, although the texture and partial semantics of the subject are preserved, the shape and outline of the subject undergo notable changes.

In fact, when calculating the cross-attention between the latent and subject features, the region outside the subject should be less focused, *i.e.*, the attention in positions outside the subject region should be suppressed. To solve this issue and ensure the precise utilization of the subject feature, we propose a **Shared Positional Embedding Anchor**, which assembles positional encoding in the calculation of *key* to effectively leverage the positional information, suppressing the phenomenon of attention dispersion, thereby concentrating attention in the subject area. Recall that the subject cross-attention is calculated by $\text{Softmax}(\frac{Q(K_{sub})^T}{\sqrt{d}})V_{sub}$, where *query* is calculated from the latent, and *key*, *value* from the subject features. We reuse the rotary positional embedding (RoPE) of the base model and add it to the subject features when mapping it to the *key* of the subject cross-attention. This operation allows the interaction between the subject features and the latent space to focus on the same local area of the subject’s contours, mitigating the influence of subject information on the global context.

5. Experiments

5.1. Setting

Datasets. To enable our training pipeline, we first collected 88K images of real-world photography. Among these, 19K images are classified as high-quality, characterized by their exceptional aesthetic quality and clear

foreground-background relationships. Subsequently, we utilized BiRefNet [52], ZoeDepth [6] and OpenCV’s built-in methods to generate accurate subject segmentation masks, depth maps and Sobel edge drafts, respectively. Next, we leveraged Hunyuan-Vision to create rich image descriptions, including spatial relationships and detailed descriptions of lighting, style, and background composition. Finally, we manually removed data with unreasonable descriptions or inaccurate segmentation masks. For the evaluation, we randomly collected images of 300 everyday items. Each image is paired with the aforementioned features and three scene descriptions generated by GPT4o. Additionally, we used two random seeds for each scene description, resulting in a total of 1,800 generation tasks (300 images \times 3 prompts \times 2 seeds) for each method.

Implementation Details. Our training was conducted on 24 NVIDIA A100 GPUs, with a batch size of 5 per GPU. The learning rate was maintained at 0.0001, using a 1K-iteration warmup. To amplify training data, we dynamically cropped each image into different sizes, including 1:1, 16:9, and 9:16 aspect ratios. During evaluation, we uniformly generate images at a resolution of 1024 \times 1024 for assessment. Unless otherwise stated, we used the default parameters of each model for comparison. Note that we additionally use an internal refiner to further enhance the details of our Pinco output images without altering their layout.

Evaluation Metrics. We consider 8 metrics from four aspects: foreground consistency, text alignment, composition rationality, and image quality.

1) **Foreground Consistency:** In our inpainting scenario, it is essential to maintain the consistency of the foreground region without altering its boundaries or recharacterizing it. We employ two off-the-shelf models, *i.e.* BiRefNet and SAM2.1-Large [37] and adopt Object Extension Ratio (OER) [8] to evaluate the pixel-level difference of generated segmentation against the ground truth mask in foreground region. OER can be computed as: $OER = \frac{\sum \text{ReLU}(M_s - M_g)}{\sum M_g}$ where M_s , M_g is the generated and ground truth mask of the foreground region. The smaller the OER is, the better consistency the method has.

2) Text Alignment: We follow Imagen3 [4] to use VQAScore [26] for alignment, given its high correlation with human assessments. In addition, we utilize the Florence-2 [45] to measure the subject redundancy, as some models fail to establish semantic associations with the foreground region and have multiple repeated subjects.

3) Rationality: In many cases, it is a challenging task to generate images with reasonable compositions, resulting in issues such as object misalignment, imbalanced proportions, and spatial disarray. To address this, we leverage GPT-4o to evaluate each image based on three aspects: placement, size, and spatial relationships. Each image is scored on a scale of 1, 3, or 5, and the average score determines the rationality. The detailed prompt can be found in the appendix Sec. F.

We also evaluate FID on MSCOCO and present statistics on the trainable parameters ratio (TPR).

5.2. Comparison

We conduct both quantitative and qualitative comparisons, along with a user study, to demonstrate the superiority of our Pinco. We quantitatively compare our Pinco with seven UNet-based models: SD1.5 ControlNet inpainting [49], SDXL inpainting [36], layerdiffusion [22], PowerPaint [53], HD-Painter [31], BrushNet [21], and Kolors-inpainting [42], as well as two DiT-based models: SD3 ControlNet inpainting [14], and Flux ControlNet inpainting [13]. Additionally, we add Adobe Firefly [1] in qualitative comparison.

Quantitative Comparison. As is shown in Tab. 1, even with a smaller number of learning parameters, Pinco achieved leading results across various evaluation metrics. Our method outperforms others notably in OER scores, demonstrating its exceptional ability to maintain the subject’s shape integrity and preserve contours and details. The top-tier VQAScore and the lowest FV2Score of Pinco further highlight its outstanding capabilities in following the detailed contents of the input prompts. Finally, GPT4o awarded Pinco the highest rationality score, showing its effectiveness in accurately managing the spatial relationship between the given foreground subject and the generated content.

Qualitative Results. The qualitative comparison with previous image inpainting methods is illustrated in Fig. 4. In foreground-conditioned inpainting tasks that involve complex textual descriptions, many methods neglect to draw certain objects in the background (such as the beach chairs referenced in the prompt for the images in the 5th row). Additionally, some approaches face challenges with subject expansion, a problem particularly noticeable with the vacuum cleaner in the 6th row. Most methods also fail to adequately consider the spatial relationships between the subject and the background, leading to subjects appearing



Figure 5. Qualitative Ablation Comparisons of Pinco, Pinco-Cross, Pinco-VAE and Pinco-w/oRoPE.

disproportionately large or mispositioned within the scene (as seen with the oversized humidifier on the bed in the 4th row). In contrast, our method effectively generates coherent and detailed backgrounds that align with the provided text while successfully mitigating the issue of subject expansion. More comparisons can be found in the supplementary material.

User Study. We selected four representative competitors for this user study. A total of 31 participants took part in our experiment, with each participant evaluating 40 sets of questions. Each set included two randomly arranged side-by-side images generated by Pinco and another method. Participants were asked to select the superior image based on several criteria, including foreground consistency preservation, text alignment, and overall image quality. The user vote results in Fig. 6 clearly demonstrate that Pinco is more favored by participants, as our model consistently received higher preference scores across all comparisons, indicating its effectiveness and reliability in producing high-quality inpainting results.

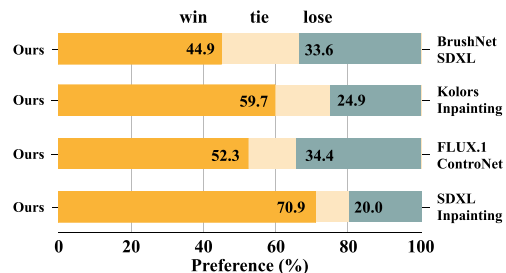


Figure 6. User Study. The images generated by Pinco received more preference from the participants compared to BrushNet [21], Kolors-IP [42], Flux-IP [13] and SDXL-IP [36].

5.3. Ablation Study

Impact of Self-Consistent Adapter injection. Fig. 5 shows that injecting subject features into the cross-attention layer can lead to three significant issues: text-driven shape expansion (illustrated in the first row of images), illogical

Table 2. Quantitative ablation study between injecting subject feature on cross-attention and self-attention layers. Injecting on the self-attention layer has a lower expand Ratio while achieving a better text alignment score.

Metrics	OER(SAM2.1) ↓	OER(BiRefNet) ↓	FV2Score ↓	Rationality ↑
Pinco (Cross)	14.55%	10.24%	3.51%	4.74
Pinco (Self)	11.51%	10.00%	3.16%	4.79

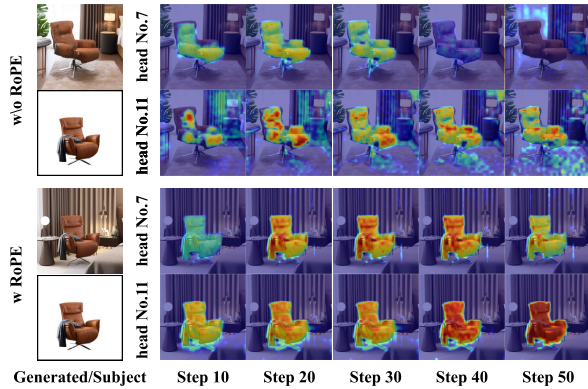


Figure 7. The attention maps of the model with rope and the model without rope. As the inference progresses, the model with RoPE gradually focuses its attention on the main subject, while the model without RoPE tends to focus on an incorrectly shaped subject and its attention map is scattered.

spatial arrangements (notably in the second row, where the washing liquid appears to float), and inadequate text alignment (as seen in the third row, which fails to include the “scattered glasses” mentioned in the prompt). The quantitative analysis presented in the Tab. 2 further highlights the advantages of incorporating in the self-attention layer, effectively mitigating shape expansion and ensuring a more coherent output. This reinforces the idea that self-attention is more aligned with the overall image layout. Furthermore, our empirical observations indicate that self-attention injection significantly boosts training efficiency and leads to much faster convergence compared to the cross-attention layer. More results are presented in the appendix Sec. E.

Impact of Decoupled Image Feature Extractor (DIFE). The comparison of the expansion rate metric is presented in Tab. 3, highlighting the performance difference between the Variational Autoencoder (VAE) and the Decoupled Image Feature Extractor (DIFE) as feature encoder. Notably, the use of DIFE results in a significant reduction in the OER(SAM2.1), decreasing it by 24.6% compared to the VAE approach. Additionally, the OER(BiRefNet) is also reduced by 4.58% when employing DIFE. Furthermore, the visual comparison in Fig. 5 reveals that relying solely on VAE for extracting subject features tends to have noticeable shape expansion. This observation affirms the effectiveness of DIFE in mitigating such issues, highlighting its advantages in maintaining the integrity of the extracted features.

Impact of Shared Positional Embedding Anchor. Fig. 5

Table 3. Object Expand Ratio comparison between using VAE only and using Decoupled Image Feature Extractor(DIFE) to extract features from subject images.

Metrics	OER(SAM2.1) ↓	OER(BiRefNet) ↓
Pinco (VAE only)	36.11%	14.58%
Pinco (DIFE)	11.51%	10.00%

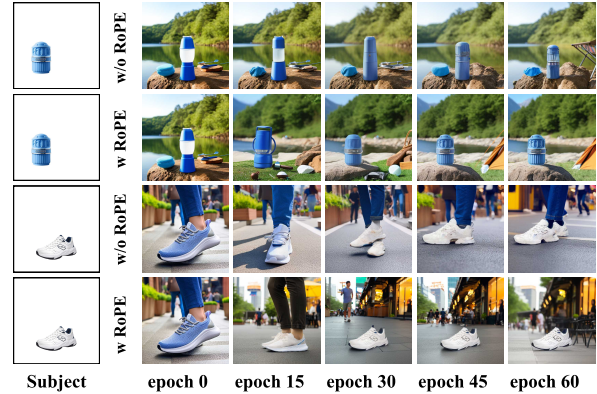


Figure 8. The convergence process of Pinco with RoPE and without RoPE. Without the help of a positional embedding anchor, the model fails to converge and can not generate an image of the correct subject.

illustrates that in the absence of a shared positional embedding anchor, the generated images primarily retain the subject’s color distribution and abstract semantic information, while the subject’s shape and texture are largely compromised. A closer examination of the attention maps in Fig. 7 reveals a phenomenon of attention dispersion when position embedding is not utilized. This suggests that the model tends to focus on global features, neglecting the local shape details of the subject. In contrast, the attention map of the model that incorporates the shared positional embedding anchor is well-aligned with the subject’s outline. Additionally, as shown in Fig. 8, the model with the positional embedding anchor effectively concentrates on the subject area when injecting subject features, leading to a significant improvement in consistency and convergence efficiency.

6. Conclusion

In this paper, we introduce Pinco, a novel plug-and-play adapter for diffusion transformers in foreground-conditioned inpainting. Pinco effectively addresses the challenges of generating high-quality backgrounds while preserving the consistency of the foreground subject. Our proposed Self-Consistent Adapter facilitates a harmonious interaction between foreground features and the overall image layout, mitigating conflicts that can arise from text and subject discrepancies. The Decoupled Image Feature Extraction method leverages distinct architectures to capture both semantic and shape features, achieving improved fea-

ture extraction and fidelity in shape preservation. Additionally, the Shared Positional Embedding Anchor allows for a more precise focus on the subject region, further enhancing the model’s performance and training efficiency. Extensive experimental results confirm that Pinco outperforms existing methods, providing a robust solution for high-quality foreground-conditioned inpainting with good text alignment and subject shape preservation.

References

- [1] Adobe firefly, 2023. Accessed: 2023-10-04. [2](#), [7](#), [14](#)
- [2] Omri Avrahami, Dani Lischinski, and Ohad Fried. Blended diffusion for text-driven editing of natural images. In *Proceedings of the IEEE/CVF conference on computer vision and pattern recognition*, pages 18208–18218, 2022. [2](#), [3](#)
- [3] Omri Avrahami, Ohad Fried, and Dani Lischinski. Blended latent diffusion. *ACM transactions on graphics (TOG)*, 42(4):1–11, 2023. [2](#), [3](#)
- [4] Jason Baldridge, Jakob Bauer, Mukul Bhutani, Nicole Brich-tova, Andrew Bunner, Kelvin Chan, Yichang Chen, Sander Dieleman, Yuqing Du, Zach Eaton-Rosen, et al. Imagen 3. [arXiv preprint arXiv:2408.07009](#), 2024. [7](#)
- [5] Fan Bao, Shen Nie, Kaiwen Xue, Yue Cao, Chongxuan Li, Hang Su, and Jun Zhu. All are worth words: A vit backbone for diffusion models, 2023. [12](#)
- [6] Shariq Farooq Bhat, Reiner Birkel, Diana Wofk, Peter Wonka, and Matthias Müller. Zoedepth: Zero-shot transfer by combining relative and metric depth. [arXiv preprint arXiv:2302.12288](#), 2023. [6](#)
- [7] Hila Chefer, Yuval Alaluf, Yael Vinker, Lior Wolf, and Daniel Cohen-Or. Attend-and-excite: Attention-based semantic guidance for text-to-image diffusion models. *ACM Transactions on Graphics (TOG)*, 42(4):1–10, 2023. [3](#)
- [8] Binghui Chen, Chongyang Zhong, Wangmeng Xiang, Yifeng Geng, and Xuansong Xie. Virtualmodel: Generating object-id-retentive human-object interaction image by diffusion model for e-commerce marketing. [arXiv preprint arXiv:2405.09985](#), 2024. [6](#)
- [9] Hong Chen, Yipeng Zhang, Simin Wu, Xin Wang, Xuguang Duan, Yuwei Zhou, and Wenwu Zhu. Disenbooth: Identity-preserving disentangled tuning for subject-driven text-to-image generation. [arXiv preprint arXiv:2305.03374](#), 2023. [3](#)
- [10] Junsong Chen, Jincheng Yu, Chongjian Ge, Lewei Yao, Enze Xie, Yue Wu, Zhongdao Wang, James Kwok, Ping Luo, Huchuan Lu, et al. Pixart-alpha: Fast training of diffusion transformer for photorealistic text-to-image synthesis. [arXiv preprint arXiv:2310.00426](#), 2023. [2](#), [3](#)
- [11] Xi Chen, Lianghua Huang, Yu Liu, Yujun Shen, Deli Zhao, and Hengshuang Zhao. Anydoor: Zero-shot object-level image customization. In *Proceedings of the IEEE/CVF Conference on Computer Vision and Pattern Recognition*, pages 6593–6602, 2024. [3](#)
- [12] Ciprian Corneanu, Raghudeep Gadde, and Aleix M Martinez. Latentpaint: Image inpainting in latent space with diffusion models. In *Proceedings of the IEEE/CVF Winter Conference on Applications of Computer Vision*, pages 4334–4343, 2024. [2](#), [3](#)
- [13] AliMama Creative. Flux.1-dev controlnet inpainting beta, 2024. Accessed: 2023-10. [2](#), [3](#), [7](#), [14](#)
- [14] AliMama Creative. Sd3 controlnet inpainting, 2024. Accessed: 2024-09. [7](#), [14](#)
- [15] Adham Elarabawy, Harish Kamath, and Samuel Denton. Direct inversion: Optimization-free text-driven real image editing with diffusion models. [arXiv preprint arXiv:2211.07825](#), 2022. [3](#)
- [16] Patrick Esser, Sumith Kulal, Andreas Blattmann, Rahim Entezari, Jonas Müller, Harry Saini, Yam Levi, Dominik Lorenz, Axel Sauer, Frederic Boesel, et al. Scaling rectified flow transformers for high-resolution image synthesis. In *Forty-first International Conference on Machine Learning*, 2024. [3](#)
- [17] Rinon Gal, Yuval Alaluf, Yuval Atzmon, Or Patashnik, Amit H Bermano, Gal Chechik, and Daniel Cohen-Or. An image is worth one word: Personalizing text-to-image generation using textual inversion. [arXiv preprint arXiv:2208.01618](#), 2022. [3](#)
- [18] Runze He, Kai Ma, Linjiang Huang, Shaofei Huang, Jialin Gao, Xiaoming Wei, Jiao Dai, Jizhong Han, and Si Liu. Freeedit: Mask-free reference-based image editing with multi-modal instruction. [arXiv preprint arXiv:2409.18071](#), 2024. [2](#), [3](#)
- [19] Amir Hertz, Ron Mokady, Jay Tenenbaum, Kfir Aberman, Yael Pritch, and Daniel Cohen-Or. Prompt-to-prompt image editing with cross attention control. [arXiv preprint arXiv:2208.01626](#), 2022. [3](#)
- [20] Yi Huang, Jiancheng Huang, Yifan Liu, Mingfu Yan, Jiayi Lv, Jianzhuang Liu, Wei Xiong, He Zhang, Shifeng Chen, and Liangliang Cao. Diffusion model-based image editing: A survey. [arXiv preprint arXiv:2402.17525](#), 2024. [2](#)
- [21] Xuan Ju, Xian Liu, Xintao Wang, Yuxuan Bian, Ying Shan, and Qiang Xu. Brushnet: A plug-and-play image inpainting model with decomposed dual-branch diffusion. [arXiv preprint arXiv:2403.06976](#), 2024. [2](#), [3](#), [5](#), [7](#), [14](#)
- [22] Pengzhi Li, Qinxuan Huang, Yikang Ding, and Zhiheng Li. Layerdiffusion: Layered controlled image editing with diffusion models. In *SIGGRAPH Asia 2023 Technical Communications*, pages 1–4, 2023. [7](#), [14](#)
- [23] Yijun Li, Sifei Liu, Jimei Yang, and Ming-Hsuan Yang. Generative face completion. In *Proceedings of the IEEE conference on computer vision and pattern recognition*, pages 3911–3919, 2017. [2](#)
- [24] Zhi Li, Pengfei Wei, Xiang Yin, Zejun Ma, and Alex C Kot. Virtual try-on with pose-garment keypoints guided inpainting. In *Proceedings of the IEEE/CVF International Conference on Computer Vision*, pages 22788–22797, 2023. [2](#)
- [25] Zhimin Li, Jianwei Zhang, Qin Lin, Jiangfeng Xiong, Yanxin Long, Xincheng Deng, Yingfang Zhang, Xingchao Liu, Minbin Huang, Zedong Xiao, et al. Hunyuan-dit: A powerful multi-resolution diffusion transformer with fine-grained chinese understanding. [arXiv preprint arXiv:2405.08748](#), 2024. [3](#), [12](#)

- [26] Zhiqiu Lin, Deepak Pathak, Baiqi Li, Jiayao Li, Xide Xia, Graham Neubig, Pengchuan Zhang, and Deva Ramanan. Evaluating text-to-visual generation with image-to-text generation. In *European Conference on Computer Vision*, pages 366–384. Springer, 2025. 7
- [27] Bingyan Liu, Chengyu Wang, Tingfeng Cao, Kui Jia, and Jun Huang. Towards understanding cross and self-attention in stable diffusion for text-guided image editing. In *Proceedings of the IEEE/CVF Conference on Computer Vision and Pattern Recognition*, pages 7817–7826, 2024. 4
- [28] Zhiheng Liu, Ruili Feng, Kai Zhu, Yifei Zhang, Kecheng Zheng, Yu Liu, Deli Zhao, Jingren Zhou, and Yang Cao. Cones: Concept neurons in diffusion models for customized generation. *arXiv preprint arXiv:2303.05125*, 2023. 3
- [29] Zhiheng Liu, Yifei Zhang, Yujun Shen, Kecheng Zheng, Kai Zhu, Ruili Feng, Yu Liu, Deli Zhao, Jingren Zhou, and Yang Cao. Cones 2: Customizable image synthesis with multiple subjects. In *Proceedings of the 37th International Conference on Neural Information Processing Systems*, pages 57500–57519, 2023. 3
- [30] Andreas Lugmayr, Martin Danelljan, Andres Romero, Fisher Yu, Radu Timofte, and Luc Van Gool. Repaint: Inpainting using denoising diffusion probabilistic models. In *Proceedings of the IEEE/CVF conference on computer vision and pattern recognition*, pages 11461–11471, 2022. 2
- [31] Hayk Manukyan, Andranik Sargsyan, Barsegh Atanyan, Zhangyang Wang, Shant Navasardyan, and Humphrey Shi. Hd-painter: high-resolution and prompt-faithful text-guided image inpainting with diffusion models. *arXiv preprint arXiv:2312.14091*, 2023. 2, 3, 7, 14
- [32] Ron Mokady, Amir Hertz, Kfir Aberman, Yael Pritch, and Daniel Cohen-Or. Null-text inversion for editing real images using guided diffusion models. In *Proceedings of the IEEE/CVF Conference on Computer Vision and Pattern Recognition*, pages 6038–6047, 2023. 3
- [33] Chong Mou, Xintao Wang, Liangbin Xie, Yanze Wu, Jian Zhang, Zhongang Qi, and Ying Shan. T2i-adapter: Learning adapters to dig out more controllable ability for text-to-image diffusion models. In *Proceedings of the AAAI Conference on Artificial Intelligence*, pages 4296–4304, 2024. 3
- [34] William Peebles and Saining Xie. Scalable diffusion models with transformers. In *Proceedings of the IEEE/CVF International Conference on Computer Vision*, pages 4195–4205, 2023. 3
- [35] William Peebles and Saining Xie. Scalable diffusion models with transformers. In *Proceedings of the IEEE/CVF International Conference on Computer Vision*, pages 4195–4205, 2023. 3
- [36] Dustin Podell, Zion English, Kyle Lacey, Andreas Blattmann, Tim Dockhorn, Jonas Müller, Joe Penna, and Robin Rombach. Sdxl: Improving latent diffusion models for high-resolution image synthesis. *arXiv preprint arXiv:2307.01952*, 2023. 2, 3, 5, 7, 14
- [37] Nikhila Ravi, Valentin Gabeur, Yuan-Ting Hu, Ronghang Hu, Chaitanya Ryali, Tengyu Ma, Haitham Khedr, Roman Rädle, Chloe Rolland, Laura Gustafson, Eric Mintun, Junting Pan, Kalyan Vasudev Alwala, Nicolas Carion, Chao-Yuan Wu, Ross Girshick, Piotr Dollár, and Christoph Feichtenhofer. Sam 2: Segment anything in images and videos. *arXiv preprint arXiv:2408.00714*, 2024. 6
- [38] Robin Rombach, Andreas Blattmann, Dominik Lorenz, Patrick Esser, and Björn Ommer. High-resolution image synthesis with latent diffusion models, 2021. 3
- [39] Robin Rombach, Andreas Blattmann, Dominik Lorenz, Patrick Esser, and Björn Ommer. High-resolution image synthesis with latent diffusion models. In *Proceedings of the IEEE/CVF conference on computer vision and pattern recognition*, pages 10684–10695, 2022. 2, 3, 4
- [40] Nataniel Ruiz, Yuanzhen Li, Varun Jampani, Yael Pritch, Michael Rubinstein, and Kfir Aberman. Dreambooth: Fine tuning text-to-image diffusion models for subject-driven generation. In *Proceedings of the IEEE/CVF conference on computer vision and pattern recognition*, pages 22500–22510, 2023. 3
- [41] Jianlin Su, Murtadha Ahmed, Yu Lu, Shengfeng Pan, Wen Bo, and Yunfeng Liu. Roformer: Enhanced transformer with rotary position embedding. *Neurocomputing*, 568:127063, 2024. 4
- [42] Kolors Team. Kolors: Effective training of diffusion model for photorealistic text-to-image synthesis. *arXiv preprint*, 2024. 7, 14
- [43] Narek Tumanyan, Michal Geyer, Shai Bagon, and Tali Dekel. Plug-and-play diffusion features for text-driven image-to-image translation. In *Proceedings of the IEEE/CVF Conference on Computer Vision and Pattern Recognition*, pages 1921–1930, 2023. 4
- [44] Qixun Wang, Xu Bai, Haofan Wang, Zekui Qin, Anthony Chen, Huaxia Li, Xu Tang, and Yao Hu. Instantid: Zero-shot identity-preserving generation in seconds. *arXiv preprint arXiv:2401.07519*, 2024. 4
- [45] Bin Xiao, Haiping Wu, Weijian Xu, Xiyang Dai, Houdong Hu, Yumao Lu, Michael Zeng, Ce Liu, and Lu Yuan. Florence-2: Advancing a unified representation for a variety of vision tasks. In *Proceedings of the IEEE/CVF Conference on Computer Vision and Pattern Recognition*, pages 4818–4829, 2024. 7
- [46] Xiangtian Xue, Jiasong Wu, Youyong Kong, Lotfi Senhadji, and Huazhong Shu. St-ldm: A universal framework for text-grounded object generation in real images, 2024. 12
- [47] Siyuan Yang, Lu Zhang, Liqian Ma, Yu Liu, JingJing Fu, and You He. Magicremover: Tuning-free text-guided image inpainting with diffusion models. *arXiv preprint arXiv:2310.02848*, 2023. 2, 3
- [48] Hu Ye, Jun Zhang, Sibio Liu, Xiao Han, and Wei Yang. Ip-adapter: Text compatible image prompt adapter for text-to-image diffusion models. *arXiv preprint arXiv:2308.06721*, 2023. 2, 3, 4
- [49] Lvmin Zhang, Anyi Rao, and Maneesh Agrawala. Adding conditional control to text-to-image diffusion models. In *Proceedings of the IEEE/CVF International Conference on Computer Vision*, pages 3836–3847, 2023. 2, 3, 4, 7, 14
- [50] Lvmin Zhang, Anyi Rao, and Maneesh Agrawala. Adding conditional control to text-to-image diffusion models. In

Proceedings of the IEEE/CVF International Conference on Computer Vision, pages 3836–3847, 2023. [2](#), [3](#)

- [51] Renrui Zhang, Jiaming Han, Chris Liu, Peng Gao, Aojun Zhou, Xiangfei Hu, Shilin Yan, Pan Lu, Hongsheng Li, and Yu Qiao. Llama-adapter: Efficient fine-tuning of language models with zero-init attention. arXiv preprint arXiv:2303.16199, 2023. [5](#)
- [52] Peng Zheng, Dehong Gao, Deng-Ping Fan, Li Liu, Jorma Laaksonen, Wanli Ouyang, and Nicu Sebe. Bilateral reference for high-resolution dichotomous image segmentation. arXiv preprint arXiv:2401.03407, 2024. [6](#)
- [53] Junhao Zhuang, Yanhong Zeng, Wenran Liu, Chun Yuan, and Kai Chen. A task is worth one word: Learning with task prompts for high-quality versatile image inpainting. arXiv preprint arXiv:2312.03594, 2023. [2](#), [3](#), [5](#), [7](#), [14](#)

Pinco: Position-induced Consistent Adapter for Diffusion Transformer in Foreground-conditioned Inpainting

Supplementary Material

A. Overview

In this supplementary material, we mainly present the following components:

- More implementation details of our model structure and training in Sec. B.
- More ablation study on the convergence of training in Sec. C.
- More details and cases of the user study in Sec. D.
- More qualitative comparisons between our Pinco and previous methods in Sec. E.
- More details and results of the GPT-4o rationality analysis in Sec. F.
- Image copyright in Sec. G

B. Implementation details

B.1. Model Architecture

Backbone We adapt the architecture proposed in Hunyuan-DiT [25] as our backbone. We use the $DiT - g/2$ config which consists of 40 blocks and has a 1408 embed_dim.

Decoupled Image Feature Extractor We use the VAE Encoder of the original Hunyuan-DiT model as our semantic feature extractor and only take the output of final layer as our semantic feature. Meanwhile, we also construct a simple convolutional network (ConvNet) to extract the shape feature. More precisely, since Hunyuan-DiT draws inspiration from the ideas of U-ViT [5] by using skip connections to link the blocks of DiT, we believe that the presence of skip connections allows different blocks to have varying granularities. If we directly feed the output of the last layer of the ConvNet into all modules without distinction, it would weaken the model’s inherent perception of feature granularity. Therefore, we extract the outputs from different layers of the ConvNet for different blocks. Specifically:

- The ConvNet consists of 7 convolutional layers, with the outputs of the 1st, 3rd, 5th, and 7th convolutional layers serving as features.
- We divided the 40 blocks into 8 groups, with each group containing 5 blocks. Considering the skip connections, we feed the features from the first layer of the ConvNet into blocks 1-5 and 36-40, and the features from the second layer into blocks 6-10 and 31-35, and so on.

Self-Consistent Adapter Since the backbone consists of 40 blocks, we construct corresponding adapters for each block to inject the subject feature. Each adapter first rearranges the feature shape to match the intrinsic latent shape [46] and then uses a linear layer to transform features from a

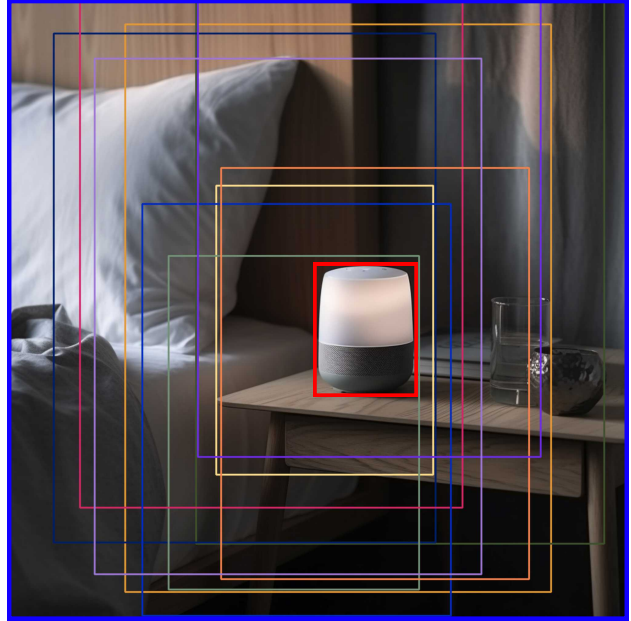


Figure 9. Method for obtaining multi-frame samples.

dimension of dim to a dimension of 1408. Then, it uses two independent matrices to obtain K and V , which are used to compute the cross-attention. The Q is directly taken from the model’s computation of self-attention.

B.2. Multi-Frame and Multi-Scale training

Due to the varying proportions of subjects within the frame—such as a vehicle that may occupy more than half of the frame, while an item like a shoe might only take up about 10%—it is essential for the model to effectively handle different frame types and generate a suitable background perspective for subjects of varying sizes. To achieve this, we employ a multi-frame augmentation method to construct training samples throughout the training process. As illustrated in Fig. 9, for each high-quality image, we define the minimum bounding rectangle of the subject based on the mask (in red), while the bounding rectangle of the entire image serves as the maximum range (in blue). We designate the areas of the maximum and minimum frames as the upper and lower bounds of a normal distribution, respectively. During training, we sample various shapes and locations of bounding rectangles to create training samples with diverse frame proportions. Fig. 12 shows more cases generated by Pinco in different scales.

Question:

Task Description:
 Analyze the physical relationship between the [subject] and the given image. Utilize your visual abilities and understanding of the physical world to assess the realism of the image and provide a brief explanation.

Evaluation Guidelines:
 Specifically, please evaluate the following aspects and score each item according to the rating criteria:
 1. **Object Placement Relationship:** Check whether the spatial relationship between the [subject] and other objects in the image is reasonable and consistent with common placement methods in daily life. Determine whether the [subject] is placed in a physically impossible position, such as floating.
 2. **Object Size Relationship:** Assess whether the size proportions between the [subject] and other objects in the image are realistic, and whether there is any disproportion between the [subject] and surrounding objects.
 3. **Physical Space Relationship:** Consider whether the spatial distance between the [subject] and other objects in the image is reasonable, whether the perspective relationship conforms to the laws of the physical world, and whether there are any unreasonable aspects.

Rating Criteria:
 - 1 point: Obvious errors, inconsistent with the real world.
 - 3 points: Minor errors, somewhat inconsistent with the real world.
 - 5 points: No obvious errors, consistent with the real world.

Please evaluate the object placement relationship, object size relationship, and spatial relationship in the image, provide three scores respectively, and briefly explain your reasoning. Think step by step to arrive at the final scores.

Given Image



Subject



Reply:

1. Object Placement Relationship: 5 points
 - The placement of the bag of dog food next to the dog on the ground appears realistic. The bag is situated on the same level as the sitting dog, and it does not appear to be floating or placed in an unnatural position. This is consistent with how objects are typically placed on the ground in a real-world scenario.

2. Object Size Relationship: 5 points
 - The size proportion between the dog and the dog food bag seems realistic. The dog food bag is reasonably large, similar to what would be expected for a product of that nature, and it does not appear disproportionately large or small compared to the dog.

3. Physical Space Relationship: 5 points
 - The spatial distance and perspective between the dog and the dog food bag appear natural. The shadows and lighting are consistent with the positioning of the objects relative to one another. This suggests a reasonable perspective and physical space relationship that conforms to the laws of the physical world.

Overall, the image presents a realistic depiction of the physical relationship between the bag of dog food and the surrounding elements. Therefore, it receives full scores in all evaluation categories

Figure 10. GPT-4o prompt for assessment and its reply. Note that you need to specify the name of the subject in [subject]

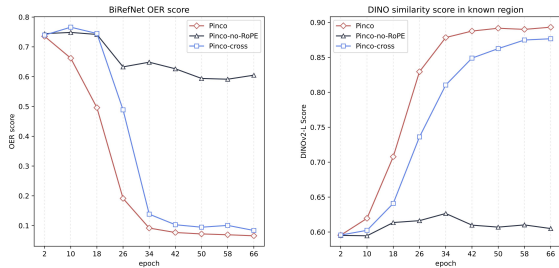


Figure 11. The convergence analysis of Pinco, Pinco-w/oRoPE, and Pinco-Cross. Pinco-Self can maintain better shape constraints and foreground consistency while achieving efficient training.

C. More Ablation Study

C.1. Convergence Process Analysis

Fig. 11 shows the convergence analysis of Pinco, Pinco-w/oRoPE, and Pinco-Cross. The two images illustrate the changes in image OER and DINO similarity within mask area as the training epochs extended. Evidently, without the aid of shared positional embedding anchor, the model struggles to effectively incorporate subject features, resulting in

consistently poor scores for both OER and DINO similarity. This highlights the importance of shared positional encoding in effectively utilizing subject features and ensuring the consistency of the subjects in the generated images. On the other hand, injecting subject features in the self-attention layer leads to faster convergence during training, with lower OER and better DINO similarity compared to injecting features in the cross-attention layer. This further supports the rationale and effectiveness of injecting features in the self-attention layer. Fig. 13 demonstrates more cases between Pinco and Pinco-w/oRoPE during the training process.

D. User Study

During the user study, participants were asked to evaluate side-by-side samples from multiple aspects, including the rationality of the background, the appropriateness of object sizes, the suitability of object placements, and the harmony between the subjects and the background, and select the images they considered to be better. Fig. 14 displays some cases from the user study.

E. More Qualitative Comparisons

We offer more qualitative comparisons between our Pinco and previous methods: SD1.5 ControlNet inpainting [49], SDXL inpainting [36], layerdiffusion [22], PowerPaint [53], HD-Painter [31], BrushNet [21], Kolors-inpainting [42], Adobe Firefly [1], SD3 ControlNet inpainting [14], and Flux ControlNet inpainting [13] in Fig. 15, 16 and 17.

F. GPT-4o Rationality

We leverage the GPT-4o to evaluate each image based on Object Placement Relationship, Object Size Relationship, and Physical Space Relationship. The criteria for these three aspects and rating criteria are as follows:

- Object Placement Relationship: Check whether the spatial relationship between the subject and other objects in the image is reasonable and consistent with common placement methods in daily life. Determine if the subject is placed in a physically impossible position, such as floating.
- Object Size Relationship: Assess whether the size proportions between the subject and other objects in the image are realistic and whether there is any disproportion between the subject and surrounding objects.
- Physical Space Relationship: Consider whether the spatial distance between the subject and other objects in the image is reasonable, whether the perspective relationship conforms to the laws of the physical world, and whether there are any unreasonable aspects.
- Rating Criteria: 1 point: Obvious errors, inconsistent with the real world. 3 points: Minor errors, somewhat inconsistent with the real world. 5 points: No obvious errors, consistent with the real world.

Fig. 18 presents the results of the rationality analysis for the images returned by GPT-4o under the criteria mentioned above. The prompt given to GPT-4o and the reply are shown in Fig. 10.

G. Copyright

Some of the images presented in this paper are sourced from publicly available online resources. In our usage context, we have uniformly retained only the main subject of the original images and removed the background parts. In this section, we specify the exact sources of the images in the form of image links and author credits in Tab. 4. Except for the images explicitly credited with the author and source, all other images are derived from client cases or generated by open-sourced models. The copyright of the images belongs to the original authors and brands. **The images used in this paper are solely for academic research purposes and are only used to test the effectiveness of algorithms.**

They are not intended for any commercial use or unauthorized distribution.

For each image containing multiple sub-images, we number them in order from left to right and from top to bottom. For example, in Figure. 1, the sub-images in the first row are numbered as SubFig.1-1, SubFig.1-2, and so on, while the sub-images in the second row are numbered as SubFig.1-5, and so forth.

Table 4. Copyright of the images in our paper.

Figure	Source
Figure. 1	SubFig.1-2 (ANTA), SubFig.1-3 (METHOU), SubFig.1-5 (BALMUDA), SubFig.1-6 (FLYCO), SubFig.1-7 (Alpha Coders)
Figure. 2	SubFig.2-1 (ZCOOL)
Figure. 3	SubFig.3-1 (Mazda)
Figure. 4	SubFig.4-1 (Foodography), SubFig.4-2 (Xiangma), SubFig.4-3 (IMAXER), SubFig.4-4 (Foodography), SubFig.4-5 (IM Motors), SubFig.4-6 (Foodography)
Figure. 5	SubFig.5-1 (NOW VISION), SubFig.5-2 (Foodography)
Figure. 7	SubFig.7-2/4 (MANTO)
Figure. 8	SubFig.8-1/2 (Foodography), SubFig.8-3/4 (LOTTO)
Figure. 10	SubFig.10-1/2 (DESING)
Figure. 12	SubFig.12-1 (MAOOXD), SubFig.12-2 (Foodography), SubFig.12-3 (Foodography), SubFig.12-4 (SUPOR), SubFig.12-5 (JianmuPhotography), SubFig.12-7 (Alpha Coders), SubFig.12-8 (BYHEALTH), SubFig.12-9 (Rarakiddo), SubFig.12-10 (Foodography), SubFig.12-11 (BALMUDA), SubFig.12-12 (LIBY), SubFig.12-13 (ROLEX), SubFig.12-14 (LUXEED), SubFig.12-15 (L'Oreal), SubFig.12-16 (Olena Bohovyk), SubFig.12-17 (BALMUDA), SubFig.12-18 (BALMUDA)
Figure. 13	SubFig.13-1 (Xiangma), SubFig.13-2 (METHOU), SubFig.13-3 (Foodography), SubFig.13-4 (NOW VISION), SubFig.13-5 (Mazda), SubFig.13-6 (JianmuPhotography), SubFig.13-7 (ANTA), SubFig.13-8 (Apple), SubFig.13-9 (Helen Keller)
Figure. 14	SubFig.14-1 (FIND VISUAL), SubFig.14-2 (Nooie Robot Vacuum), SubFig.14-3 (RIMOWA), SubFig.14-4 (XIAOMI), SubFig.14-5 (Box Studio), SubFig.14-6, SubFig.14-7 (Foodography), SubFig.14-8 (FIND VISUAL)
Figure. 15	SubFig.15-1 (Xiangma), SubFig.15-2 (METHOU), SubFig.15-3 (FILMSAYS), SubFig.15-4 (Alpha Coders)
Figure. 16	SubFig.16-2 (AUPRES), SubFig.16-3, SubFig.16-4 (MAOOXD)
Figure. 17	SubFig.17-1 (Bear), SubFig.17-2 (Luckin Coffee), SubFig.17-3 (Apple), SubFig.17-4 (FIND VISUAL)
Figure. 18	SubFig.18-2 (Foodography), SubFig.18-3 (YUANYI).

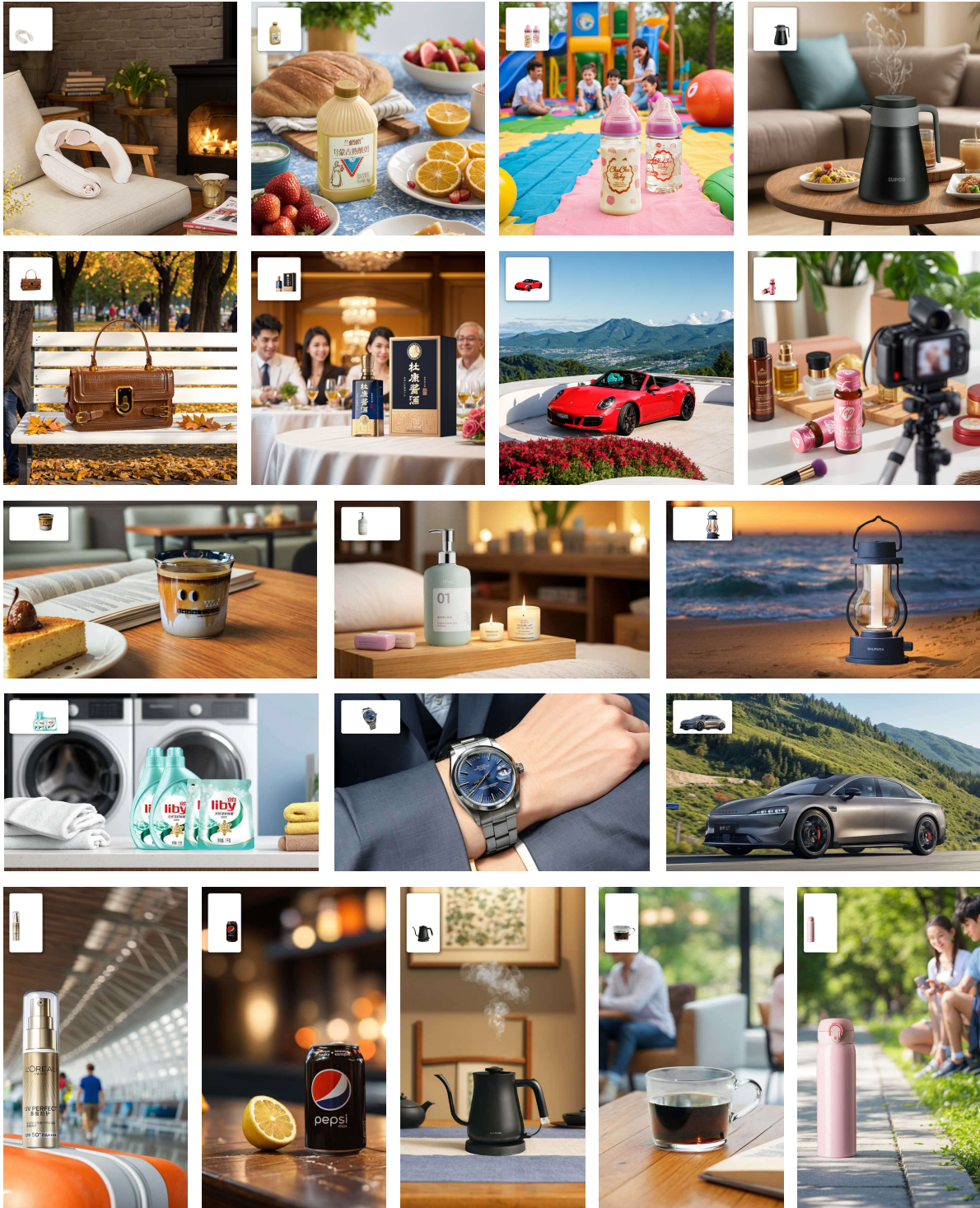


Figure 12. More cases generated by Pinco. Pinco supports the generation of high-quality images at different scales while ensuring the reasonable placement of subjects, achieving realistic foreground-conditioned inpainting

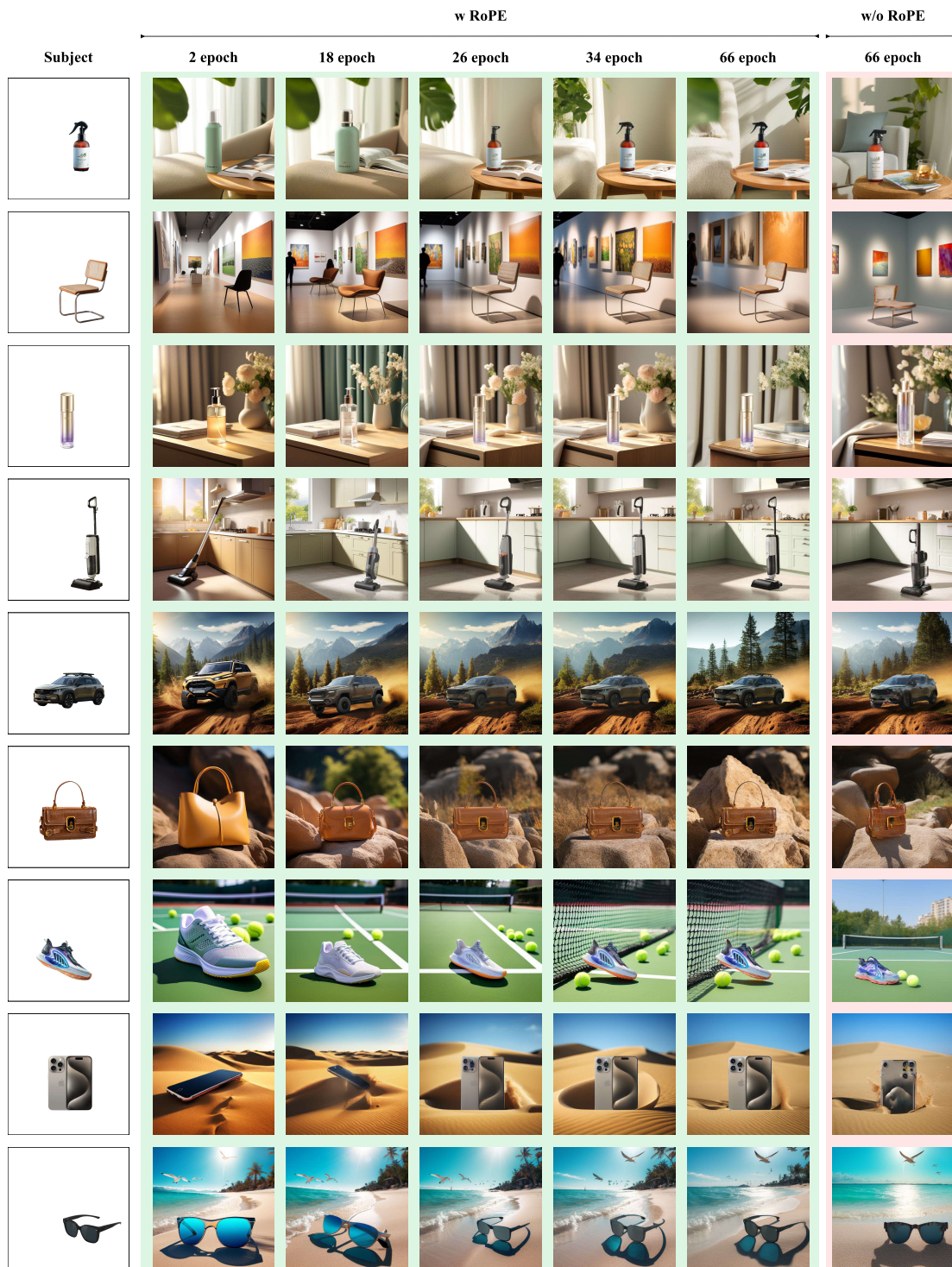


Figure 13. More cases of the model training process. We provide a detailed demonstration of the training process of the Pinco, while only presenting the final results of the Pinco-w/o RoPE due to limited space. We can observe that the Pinco model can gradually place the given subject into the generated scene while maintaining the contour and foreground consistency. In contrast, although the same number of training epochs were used, the Pinco-w/o RoPE model can only learn partial subject information, resulting in distortions in both contour and foreground consistency. Zoom in to observe the details.

A thermos, placed on the countertop of a kitchen, is set against a backdrop of elegant cabinets and tidy cooking utensils. The thermos appears both minimalist and stylish, accompanied by several fresh fruits.



A robotic vacuum cleaner is placed in the living room, with a backdrop of minimalist furniture and fresh indoor plants. The floor is clean and tidy.



A suitcase is placed in a busy airport waiting lounge, with a background featuring travelers waiting and a display screen showing boarding information.



The smart bracelet, set against an outdoor sports environment, features a backdrop of mountains and blue skies. Surrounded by grass and natural landscapes, it creates a lifestyle that is close to nature.



Orange juice, placed on an outdoor picnic blanket, with a background of lush green grass in a park. Next to the orange juice are sandwiches and fresh fruits, surrounded by happy families.



Sneakers placed in a vast mountainous and leafy outdoor environment, with distant peaks and clear lakes in the background. The sneakers tread on a firm dirt path surrounded by lush greenery.



The chopstick and bowl storage box is placed on the supermarket shelf, with its vibrant packaging attracting customers' attention. Surrounding shelves are filled with various kitchen supplies.



A blender is placed in an environment that emphasizes healthy eating, with a background of nutritious ingredients and sunlight streaming through the window.



Text Prompt

Subject

SDXL Inpainting

Kolors Inpainting

Flux-dev ControlNet

BrushNet-SDXL

Pinco (Ours)

Figure 14. Some cases in our user study.

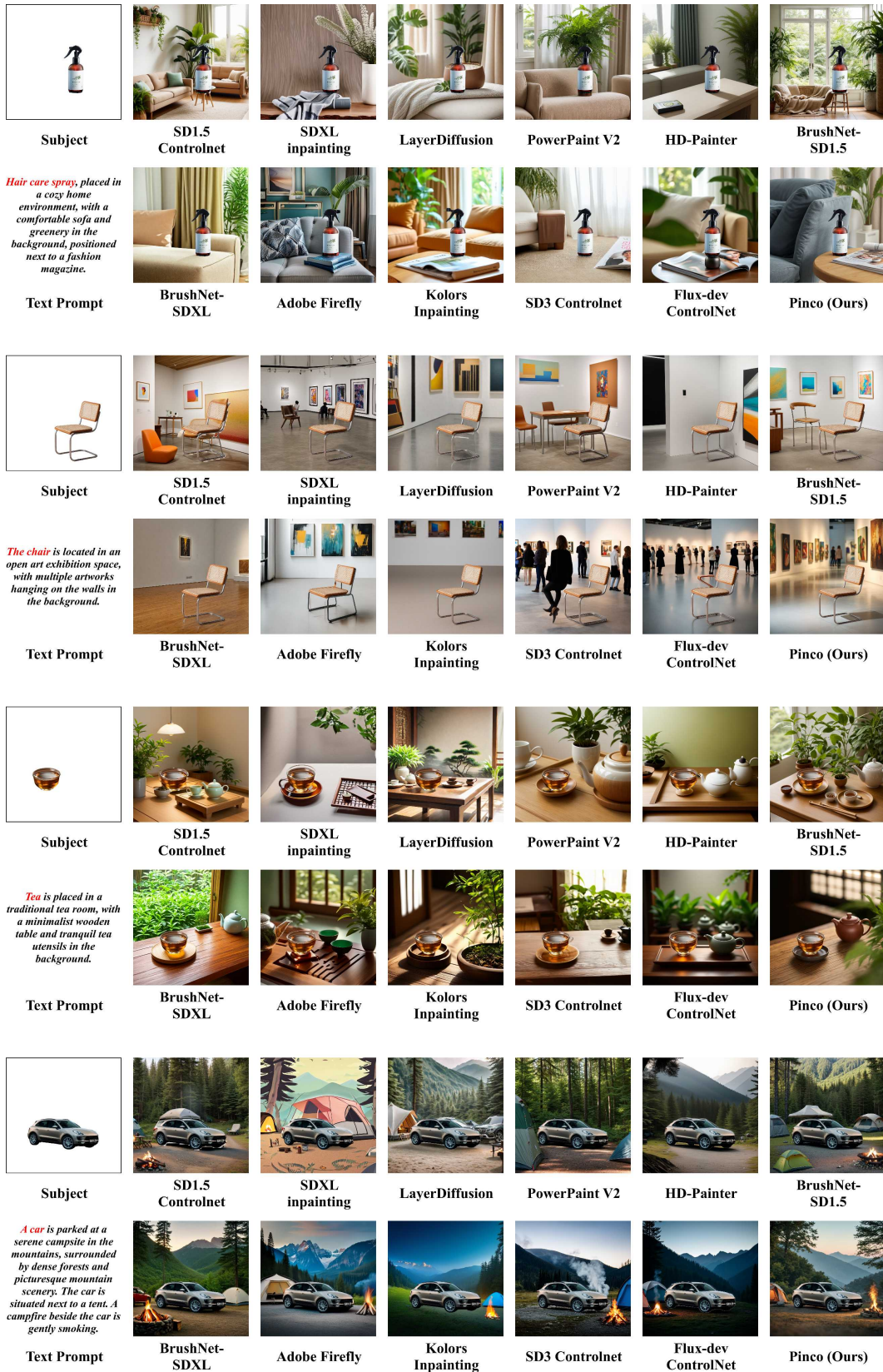


Figure 15. More qualitative comparisons between our Pinco and previous methods.

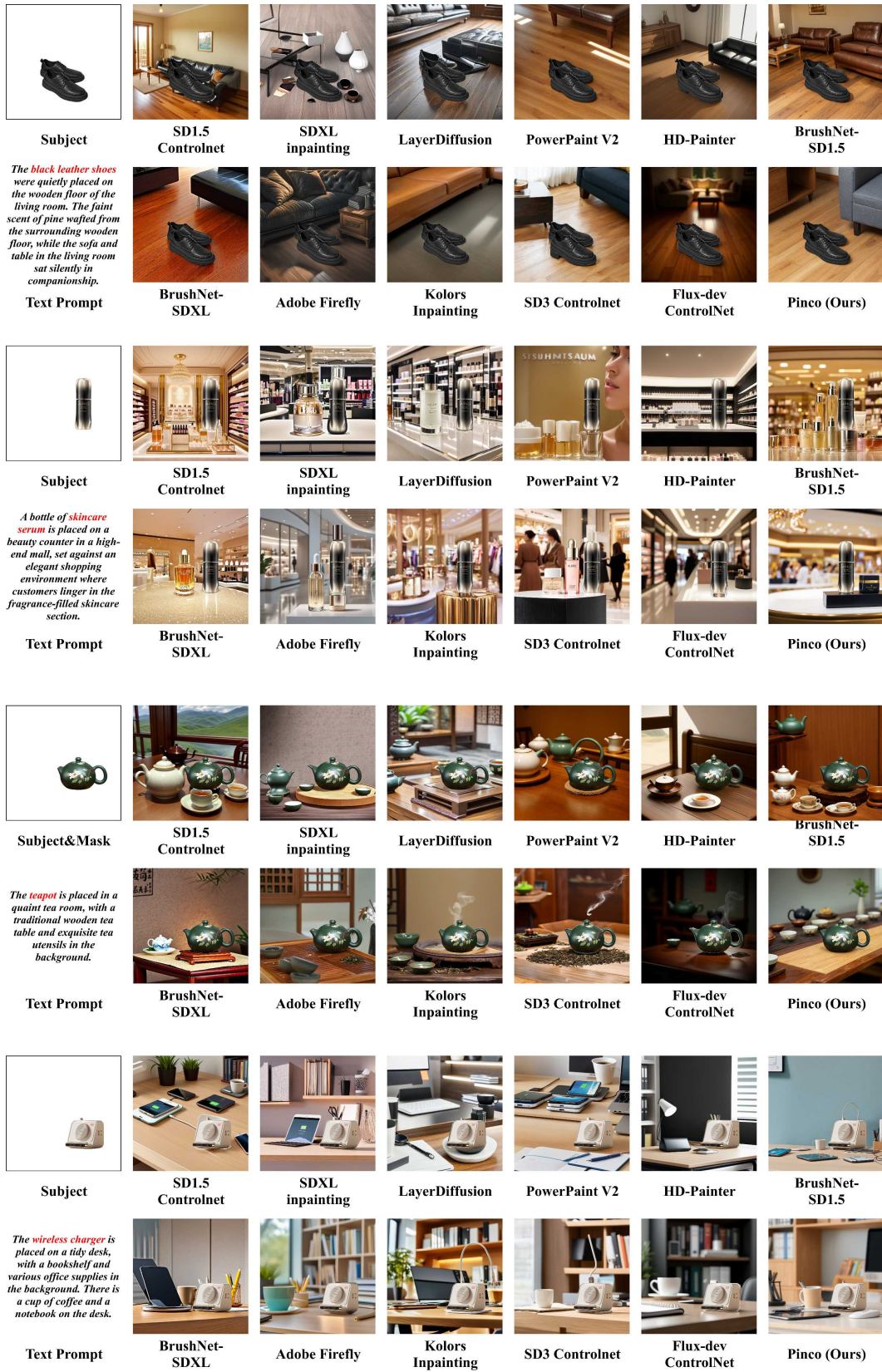


Figure 16. More qualitative comparisons between our Pinco and previous methods.

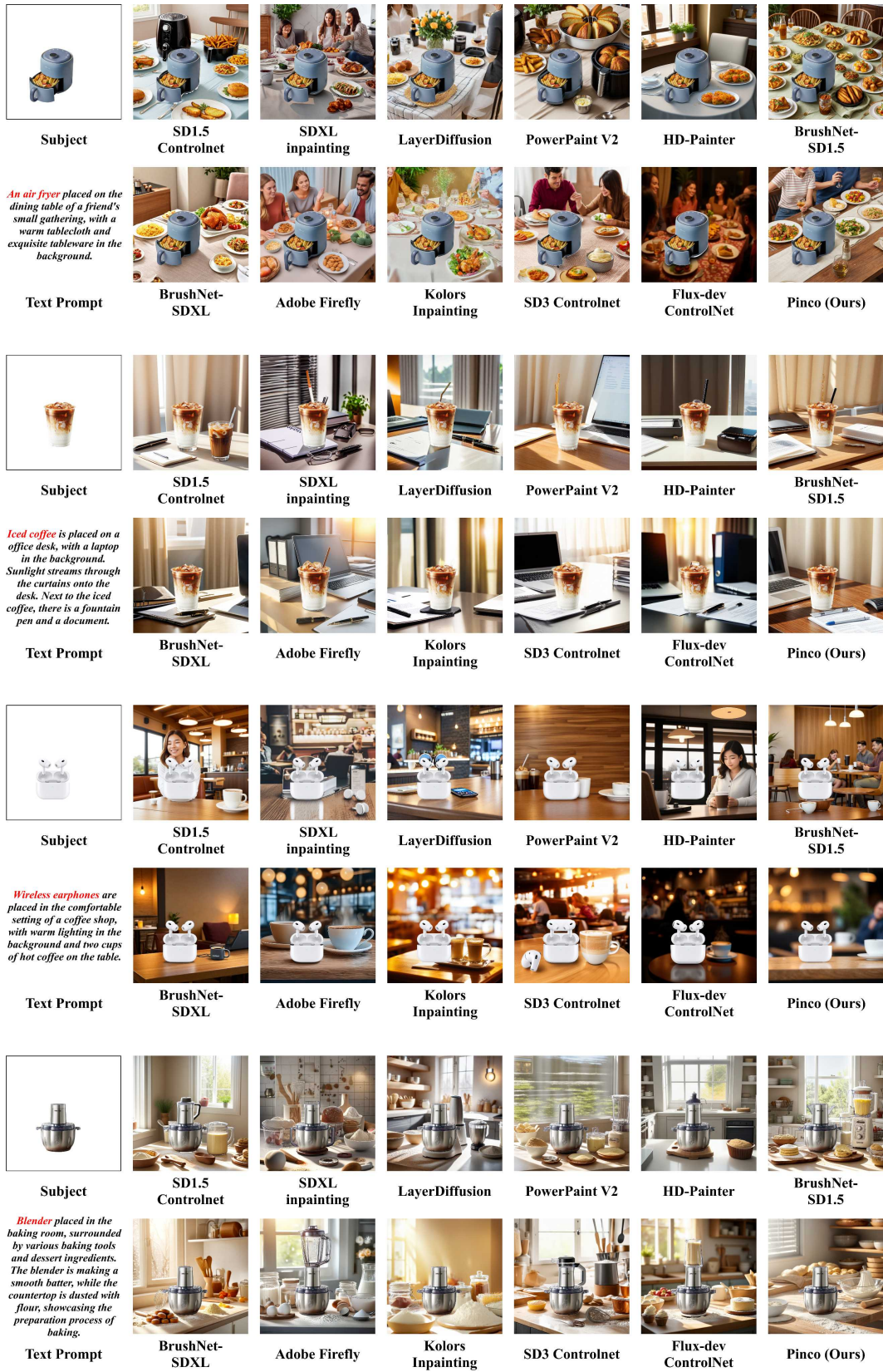


Figure 17. More qualitative comparisons between our Pinco and previous methods.

Object Placement Rationality



Subject



Score: 1.0

The electric kettle appears to be suspended above the floor and is not resting on any surface. This placement is inconsistent with its typical usage, as kettles are usually found on countertops or tables. Therefore, it seems unrealistic.



Score: 3.0

The electric kettle is placed on top of a stick inserted into a stack of books, which is an unusual and unconventional setup in a real-world context. While it does not appear to be floating and seems supported, this method of placement is not realistic.



Score: 5.0

The kettle is placed securely on a table, supported by a cloth, which is a typical and reasonable placement.

Object Size Rationality



Subject



Score: 1.0

The bottles are disproportionately large compared to the surrounding stadium and the people, suggesting a lack of realism in scale. Usually, detergent bottles are much smaller than stadiums or people.



Score: 3.0

The bottle appears larger relative to the hand pouring it, which could be slightly disproportionate depending on the context.



Score: 5.0

The size of the bottle in relation to the table and the background scene appears realistic. Compared to the people and the stadium setting, the bottle seems proportionally appropriate and does not appear disproportionately large or small.

Physical Spatial Relationship



Subject



Score: 1.0

The perspective and spatial distance between the fan and other objects, like the bed, are not realistic. The fan's position doesn't match the room layout and suggests an unusual or impossible spatial arrangement.



Score: 3.0

While the placement of the fan seems grounded on the bed, the exaggerated size creates a sense of spatial distortion, which might not conform to usual bedroom perspectives. However, there are no major discrepancies in terms of the perspective relationship.



Score: 5.0

The spatial distance between the fan and other objects, including the wall, pictures, and bed, aligns well with the perspective of the room. The perspective and spatial arrangement match common physical laws.

Figure 18. GPT-4o rationality analysis results.